Connecting Communities Through Underground Infrastructure – Eberhardt et al. (Eds)

Interpretable modeling of cutterhead torque in Earth Pressure Balance machines via Kolmogorov-Arnold networks

J. Loy-Benitez and S.S. Lee
Department of Earth Resources and Environmental Engineering, Hanyang University, Seoul, Republic of Korea

ABSTRACT: Earth pressure balance (EPB) shield machines are preferred in tunnel excavation due to their adaptability and efficiency. Given dynamic geological conditions during tunnelling often cause fluctuations in the cutterhead torque, challenging numerical models. This study proposes a Kolmogorov-Arnold network (KAN) model to estimate cutterhead torque using operational EPB parameters. Moreover, KANs showed superiority compared to state-of-the-art methods while providing interpretability. Mutual information analysis is utilized for feature selection and the jellyfish search optimization algorithm is used to fine-tune KAN hyperparameters. This integration offers a robust and interpretable framework for real-time torque estimation, supporting a more adaptive tunnel excavation under geological conditions.

1 INTRODUCTION

Earth pressure balance (EPB) shield machines are prevalent in tunnel construction due to their strong adaptability, advance speed, and short interferences (Wan et al., 2024). Given a complex geological environment and sudden changes during excavation, the machine parameters should be adjusted to match driving and soil conditions (Kim et al., 2022). Among these, the operational parameters, the cutter torque is likely to exceed the rated value in changing geological driving conditions, and limit the values of cutter speed and thrust.

Several physical models and numerical simulations have demonstrated acceptable results on modelling operational EPB parameters; however, these fail in estimating these parameters under dynamic geological conditions during the tunnel excavation (Gao et al., 2025). Recent advances have considered artificial intelligence (AI) techniques that analyse the relationship among the operating variables to enable strong generalization capabilities. These features are suitable for uncertain conditions and fuzzy environments during tunnel excavation (Loy-Benitez et al., 2024).

Shielding machine parameters are influenced by rock mass conditions, machinery specifications, and working process (Erharter et al., 2025). These influences can be leveraged by soft-computing methods to estimate relevant parameters. Over the past decade, multilayer perceptron (MLP) models have been extensively utilized for integrated management systems, considering modelling, monitoring, and control in shielding machines. However, novel techniques have been recently introduced, adding interpretability to the models, allowing operators to understand the impact and influence of machine parameters over the cutterhead torque.

Recently, the Kolmogorov-Arnold networks (KAN) have been introduced as a novel neural approach in which the activation functions need to be learned, evidencing superior performances compared to the MLP in terms of model accuracy and interpretability (Liu et al., 2024). This study aims to introduce a KAN-based cutterhead torque model considering EPB operational parameters while adding interpretability in terms of the impact of each variable on the target. In addition, mutual information (MI) analysis is utilized to select the most relevant features to

DOI: 10.1201/9781042001064-208

model the cutterhead torque. Moreover, a metaheuristic optimization algorithm (MOA), i.e., the jellyfish search optimization algorithm (JSO), is utilized to select the KAN hyperparameters that yield the most accurate torque estimations (Ramkumar et al., 2024; Sulaiman & Labadin, 2015).

2 MATERIALS AND METHODS

2.1 *Study area and data description*

The shield machine is considered an EPB working in a tunnelling project in the Seoul metropolitan area; the machine characteristics are included in Table 1. The project comprises a total tunnel alignment of approximately 1,600 m long, including seven ventilation shafts and two stations. The northern and southern running tunnels have alignment lengths are 760 m and 762 m, respectively. The EPB excavation was conducted over 1,011 segment rings, corresponding to a total excavation length of 1,522 m, excluding the station boxes and shaft sections where mechanical excavation was not performed. Moreover, the tunnel depth is relatively shallow, ranging from 6 to 20 m.

The ground composition in the departure consisted of weathered and soft rock, and at the arrival zone consisted of an alluvial zone, and the groundwater level was found to be 7 to 8 m below the surface and 3 to 4 m above the tunnel crown.

This study considers 42 EPB operational variables. These measurements were collected in a time resolution of 2 – 3 minutes, accounting for 75 – 80 observations per ring. A total of 7,936 observations were collected, and the 3σ method was utilized for outlier removal, leaving a total of 6,340 observations for training and validating the proposed method.

Table 1. Characteristics of the EPB machine.

Item	Description
Type/Supplier	Earth Pressure Balance/Hitachi Zosen (Japan)
Grouting	Upper Section 4EA, Lower Section 2EA, Chamber 4EA
Muck handling	Muck car + vertical conveyor belt, belt scale
ID/OD	7.47 m/ 7.69 m
Segment	RC-segment, L 1,500 mm + t 300 mm, 7 pieces
RPM	0.6 – 3.53 RPM, electric motor type
Torque	11,300 – 43,300 kN-m (α = 24.8)
Cutterhead	Dome type, 17-inch cutter, scraper
Thrust force	1,120 kN/m^2/52,000 kN

2.2 *Mutual information for feature selection*

The *MI* criterion is based on the probability density function (PDF) of each variable considered in the regression model. The results are scores for each feature to be ranked and selected as an optimal set of predictors for the estimation of a certain variable.

The *MI* of two random variables measures the dependence or information between them. Unlike the correlation coefficient, the *MI* approach is able to detect non-linear relationships between variables. The *MI* of random variables *X* and *Y* is defined by the PDF of *X* and *Y* and the joint (*X, Y*). The PDF of X, Y, and the joint (X, Y) are expressed as f_X, f_Y, andf_{XY}, respectively. Then, the *MI*(*X; Y*) is computed as in Equation 1 (Sulaiman & Labadin, 2015).

$$MI(X;Y) = \iint f_{X,Y}(x,y)\log\frac{f_{X,Y}(x,y)}{f_X(x)f_Y(y)}\,dx\,dy \tag{1}$$

It should be noted that if *X* and *Y* are independent, then the joint PDF is equal to the product of the PDFs of *X* and *Y*; and therefore, *MI* becomes zero.

2.3 *Kolmogorov-Arnold networks*

MLP models follow the universal approximation theorem; as an alternative, KAN models are introduced as an approach following the Kolmogorov-Arnold representation theorem. This theorem states that, considering a multivariate continuous function $f : [0, 1]^n \rightarrow$, It can be expressed as a finite composition of continuous functions of a single variable and the binary operation of addition, as expressed in Equation 2 (Liu et al., 2024).

$$f(X) = f(x_1, x_2, \ldots, x_n) = \sum_{q=1}^{2n+1} \Phi_q \left(\sum_{p=1}^{n} \varphi_{q,p}(x_p) \right) \tag{2}$$

Where $\varphi_{g_1 p,} : [0, 1] \rightarrow$ and $\Phi_q : \rightarrow$. Here, it is shown that the only true multivariate function is addition.

Nevertheless, this 2-layer width might not be smooth due to its limited expressive power. Then, it can be generalized utilizing arbitrary depths and widths written in a matrix form as in Equation 3.

$$f(x) = \Theta_{out} \circ \Theta_{in} \circ x \tag{3}$$

Where Θ_{in} and 1 Θ_{out} are expressed as in Equations 4 and 5, respectively.

$$\Theta_{in} = \begin{bmatrix} \theta_{1,1}(\cdot) & \ldots & \theta_{1,n}(\cdot) \\ \vdots & \ddots & \vdots \\ \theta_{2n+1,1}(\cdot) & \ldots & \theta_{2n+1,n}(\cdot) \end{bmatrix} \tag{4}$$

$$\Theta_{out} = (\Theta_1(\cdot) \quad \ldots \quad \Theta_{2n+1}(\cdot)) \tag{5}$$

Withal, these matrices are special cases of Θ, considering n_{in} inputs, and n_{out} outputs; then, a Kolmogorov-Arnold layer can be expressed as in Equation 6.

$$\Theta = \begin{pmatrix} \theta_{1,1}(\cdot) & \ldots & \theta_{1,n_n}(\cdot) \\ \vdots & \ddots & \vdots \\ \theta_{n_n,1}(\cdot) & \ldots & \theta_{n_n,n_n}(\cdot) \end{pmatrix} \tag{6}$$

Here, Θ_n corresponds to $n_{in} = n$, $n_{out} = 2n + 1$, and Θ_and corresponds to $n_{in} = 2n + 1$ and $n_{out} = 1$.

The KAN can be constructed by stacking layers. Assuming L layers, the l^{th} layer Θ_out have shape (n_{l+1}, n_l); then, the network is defined as in Equation 7.

$$KAN(x) = \Theta_{L-1} \circ \ldots \circ \Theta_1 \circ \Theta_0 \circ x \tag{7}$$

On the other hand, an MLP network is interleaved by linear layers w_1 and nonlinearities σ, as expressed in Equation 8.

$$MLP(x) = W_{L-1} \circ \sigma \circ \ldots \circ W_1 \circ \sigma \circ W_0 \circ x \tag{8}$$

2.4 *Jellyfish search optimization for hyperparameter selection*

This study introduces a KAN-based framework for estimating cutterhead torque using EPB operational variables. However, manually setting hyperparameters is inefficient and indicates a lack of systematic exploration. Therefore, the JSO algorithm is chosen to optimize the hyperparameters in the KAN model, including the grid, which consists of the number of grid points used to parameterize the nonlinear univariate functions. The value of k represents the degree of smoothness control, or the complexity of the nonlinear transformation, for interpolation across the grid.

Moreover, h1 and h2 represent the number of neurons or the width of the final transformations using an MLP approach. In this context, the objective function consists of minimizing the mean squared error (MSE), computed as in Equation 9.

$$MSE = \frac{1}{n}\sum_{i=1}^{n}|y - \hat{y}|^2 \tag{9}$$

The JSO algorithm works based on the search behaviour and jellyfish movement in the ocean, and consists of three rules (Ramkumar et al., 2024).

1. The jellyfish movement varies inside the ocean and with the swarm, governed by a time control mechanism that switches the jellyfish movement.
2. The jellyfish movement depends on food availability at a specific location.
3. The amount of food is determined by the location and its corresponding objective function.

2.5 *The proposed method*

Figure 1 illustrates the research framework of this study, divided into three phases. Phase 1 consists of data pre-treatment and feature selection. A total of 42 EPB variables are considered, and outliers are removed through the 3σ method. Then, *MI* is utilized for feature selection, scoring the relationship of the EPB variables with the cutterhead torque; then, considering the greatest scores, the dataset is built for subsequent model training. Then, the variables are MinMax normalized, and the dataset is split into training and test sets for model training and validation, respectively, with a ratio of 60/40.

Phase 2 consists of the KAN model training and the JSO-based hyperparameter optimization. The KAN model is structured with parameters including grid, *k*, and hidden neurons selected through the JSO for MSE minimization. Finally, phase 3 includes the performance assessment and interpretability, considering the trained and optimized model. State-of-the-art methods are introduced for comparison with the proposed methodology, and the interpretability is shown as the learn splines for each predictor to the cutterhead torque.

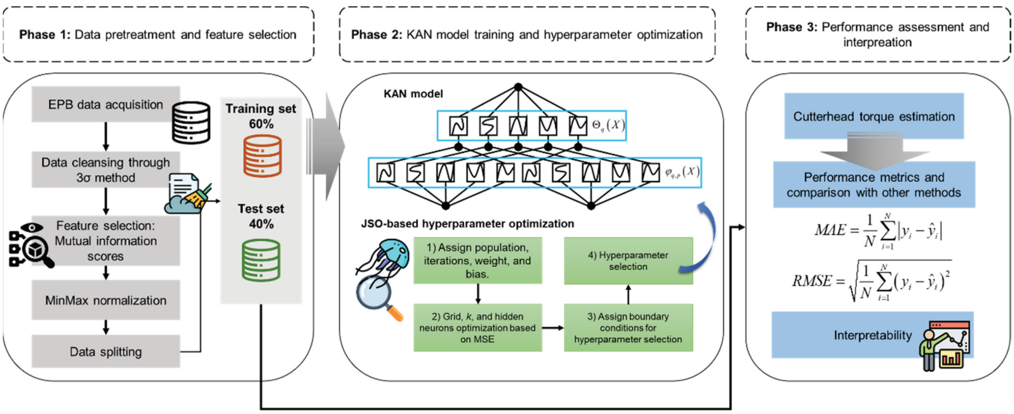

Figure 1. Flowchart of the proposed method.

3 RESULTS AND DISCUSSION

3.1 *Data pre-treatment and MI-based feature selection*

Considering the EPB operational data, the cleansing method removes three standard deviations above and below the measurements. A total of 6,340 observations were considered for the development of this study, and after data cleansing, 1,596 observations were removed. Figure 2 shows the results of the MI-based feature selection process, considering a normalized MI score denoting the predictors' relationship with the cutterhead torque. Four variables, including the cutter motor current, the cutter CCW, the cutter seal temperature, and the top earth pressure, show greater scores, i.e., strong relationships.

First, the motor current is directly related to the power required to rotate the cutterhead; the cutter CCW, related to the interaction soil/machine as the excavation progresses; the cutter seal temperature, as with the friction and load due to rotation; therefore, higher torque values can imply higher resistance and temperature rises. Finally, the top earth pressure represents the geotechnical load above the machine, in which a great overburden influences face pressure and increases the torque to maintain excavation stability.

The selected features are 12 operational variables that yielded the normalized MI scores greater than 0.2. Although three additional variables also exceeded this threshold, they were excluded from the set due to strong collinearity and redundancy with other variables. The final predictor set includes important variables related directly to the torque, including the cutterhead RPM, stroke, pressures, and screw pressure.

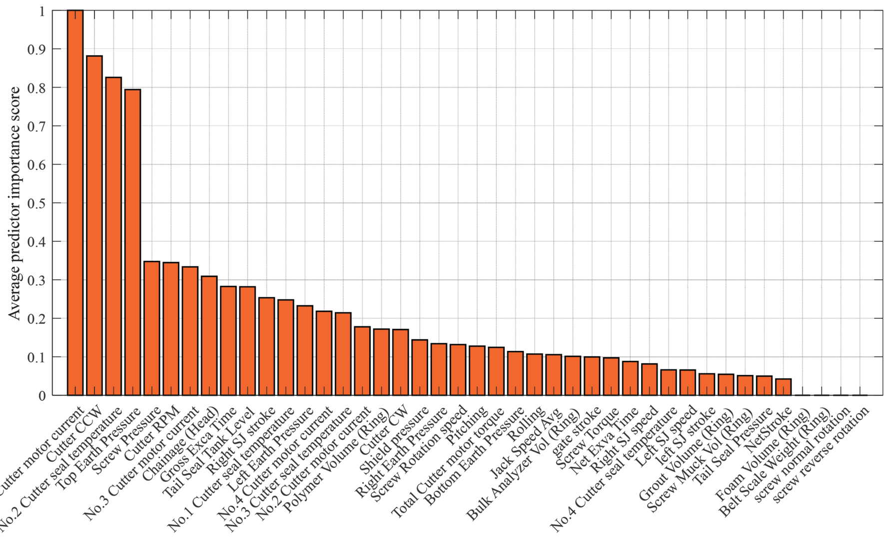

Figure 2. Results of the MI scores for feature selection.

3.2 *KAN-based modeling and hyperparameter optimization*

Training the KAN models aims to minimize the MSE considering the predicted and actual cutterhead torque values. The inputs are set to 12, and the output is set to 1 for a step ahead of the cutterhead torque measurement. Then, a backpropagation algorithm, normally utilized for MLPs, is modified considering the functional nature of the connections. Unlike MLPs, the KAN model updates the spline parameters defining each function instead of updating scalar weights.

The JSO algorithm is utilized to select the hyperparameters of the grid, k, and hidden neurons for two layers, considering the space search with boundaries as [2, 15], [2, 15], [32, 256], [32, 256], respectively. The objective function consists of the MSE, initializing the population size with 50, and a single iteration due to increased computational costs. The optimization results are shown in Figure 3a, considering the set of parameters [grid = 15, k = 2, h1 = 105, h2 = 256] as the optimal, and subsequently utilized to train the KAN model.

The KAN model was trained with the determined hyperparameters, setting a maximum number of epochs of 10,000; however, two regulators were utilized, including an early stopping with patience of 500 epochs, and a model checkpoint to save only the best model. The training process is shown in Figure 3b, where the training was stopped at epoch 630.

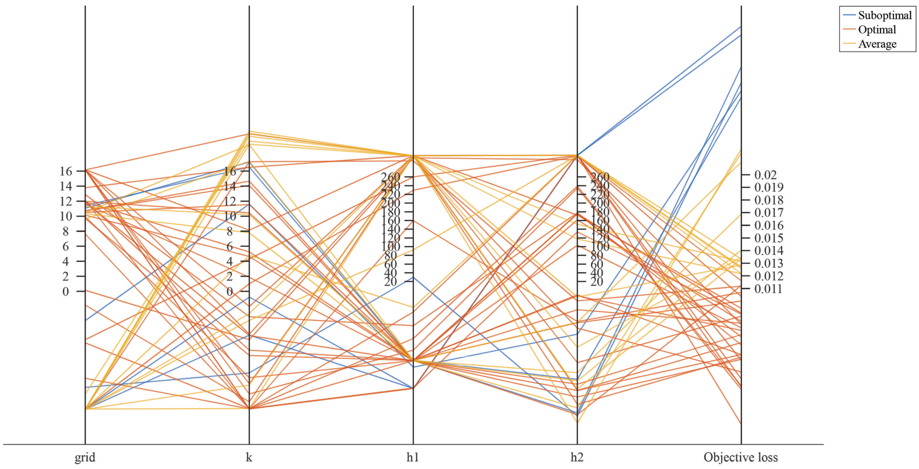

(a)

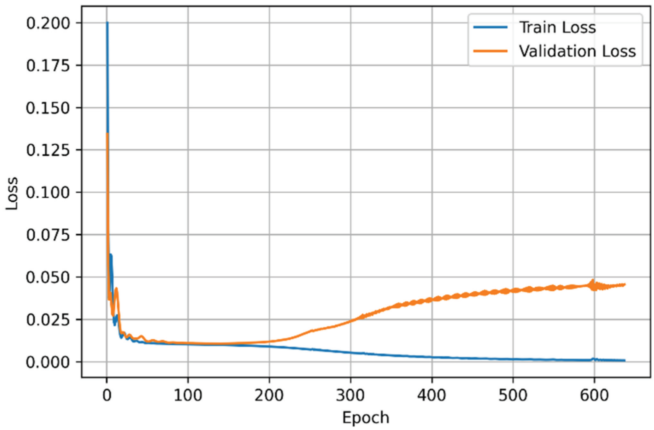

(b)

Figure 3. (a) Parallel plot for the JSO-based hyperparameter optimization, and (b) training process of the KAN model.

3.3 *Performance assessment of the proposed method*

Once the KAN model is optimized and trained, other methods are utilized to assess its performance. The state-of-the-art methods are linear regression, random forest, gradient boosting, stochastic gradient descent, and the MLP. The modelling results in time series with their residuals are illustrated in Figure 4a, while the comparison with state-of-the-art methods metrics is shown in Figure 4b. Contrary to linear and neuron methods, the approximation approach of KAN demonstrated superior accuracy.

On the other hand, Figure 5 illustrates the feature attribution of the input variables and their normalized form. Considering higher scores, the associated features are the cutter CCW, the top earth pressure, screw pressure, No. 3 cutter motor current, stroke, excavation time, and tail seal tank level. These features can serve as variables to take into account when generating control loops for the cutterhead torque. The CCW indicates reverse cutting during high-resistance events, while the top earth pressure and screw pressure represent the ground reaction force and the soil density and cohesion, respectively. Motor current is directly related to the mechanical load, and the stroke affects torque by increasing the material engagement and longer excavation times.

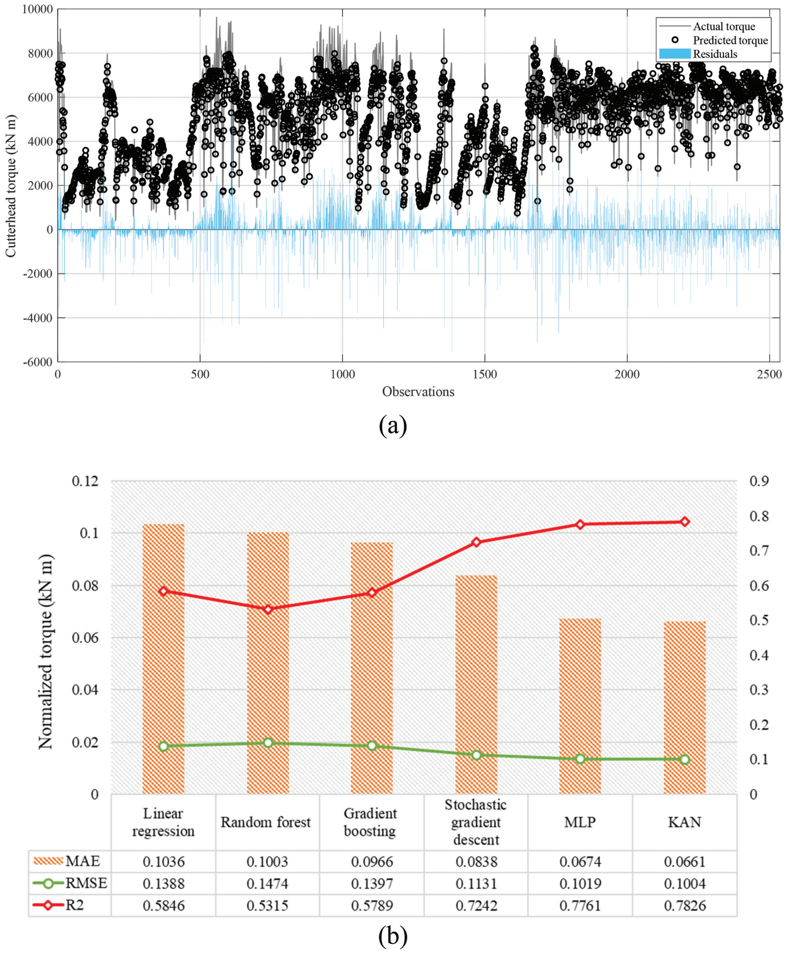

Figure 4. (a) Actual and KAN-based modelled cutterhead torque measurements with residuals, and (b) comparison of performance metrics using different methods.

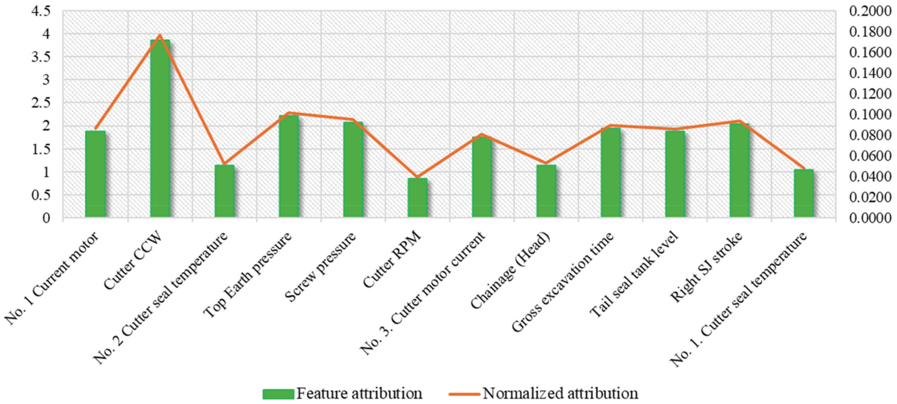

Figure 5. Feature attribution yielded by the KAN model for cutterhead torque estimation.

ACKNOWLEDGEMENTS

This work was supported by the BK21 FOUR (Fostering Outstanding Universities for Research) program (No. 4299990314624) through the National Research Foundation of Korea (NRF) funded by the Korea Ministry of Education and the Korea Institute for Advancement of Technology (KIAT) grant funded by the Korea Government (MOTIE) (RS-2024-00410787, HDR Program for Industrial Innovation).

REFERENCES

Chou, J. S., & Truong, D. N. (2021). A novel metaheuristic optimizer inspired by behavior of jellyfish in ocean. *Applied Mathematics and Computation*, 389, 125535. https://doi.org/10.1016/j.amc.2020.125535

Erharter, G. H., Unterlass, P., Radončić, N., Marcher, T., & Rostami, J. (2025). Challenges and Opportunities of Data-Driven Advance Classification for Hard Rock TBM excavations. *Rock Mechanics and Rock Engineering*, 0123456789. https://doi.org/10.1007/s00603-025-04542-4

Gao, K., Liu, S., Su, C., & Zhang, Q. (2025). A multi-stage learning method for excavation torque prediction of TBM based on CEEMD-EWT-BiLSTM hybrid network model. Measurement: *Journal of the International Measurement Confederation*, *247*(January), 116766. https://doi.org/10.1016/j.measurement.2025.116766

Kim, D., Pham, K., Oh, J. Y., Lee, S. J., & Choi, H. (2022). Classification of surface settlement levels induced by TBM driving in urban areas using random forest with data-driven feature selection. *Automation in Construction*, *135*(December 2021), 104109. https://doi.org/10.1016/j.autcon.2021.104109

Liu, Z., Wang, Y., Vaidya, S., Ruehle, F., Halverson, J., Soljačić, M., Hou, T. Y., & Tegmark, M. (2024). *KAN: Kolmogorov-Arnold Networks.* 1–50. http://arxiv.org/abs/2404.19756

Loy-Benitez, J., Kyu, M., Choi, Y., Lee, J., & Seungwon, S. (2024). Breaking new ground: Opportunities and challenges in tunnel boring machine operations with integrated management systems and artificial intelligence. *Automation in Construction*, *158*(May 2023), 105199. https://doi.org/10.1016/j.autcon.2023.105199

Ramkumar, M., Gowtham, M. S., Syed Jamaesha, S., & Vigenesh, M. (2024). Attention induced multi-head convolutional neural network organization with MobileNetv1 transfer learning and COVID-19 diagnosis using jellyfish search optimization process on chest X-ray images. *Biomedical Signal Processing and Control*, *93*(December 2023), 106133. https://doi.org/10.1016/j.bspc.2024.106133

Sulaiman, M. A., & Labadin, J. (2015). Feature selection based on mutual information for machine learning prediction of petroleum reservoir properties. *2015 9th International Conference on IT in Asia: Transforming Big Data into Knowledge, CITA 2015 - Proceedings*, 1–6. https://doi.org/10.1109/CITA.2015.7349827

Wan, Z., Li, S., Zhao, S., & Liu, R. (2024). Rheological characterization of the conditioned sandy soil under gas-loading pressure for earth pressure balance shield tunnelling. *Tunnelling and Underground Space Technology*, *146*(February), 105658. https://doi.org/10.1016/j.tust.2024.105658